Neurochemical and Neurophysiological Effects of Intravenous Administration of *N,N*-dimethyltryptamine in Rats

Abbreviated title: Neural Correlates of DMT in Rats

Nicolas G. Glynos[1-4], Emma R. Huels[2-5], Amanda Nelson[2], Youngsoo Kim[6], Robert T. Kennedy[6], George A. Mashour[2-5], Dinesh Pal[1-5*]

1. Department of Molecular & Integrative Physiology, University of Michigan, Ann Arbor, MI 48109, USA
2. Department of Anesthesiology, University of Michigan, Ann Abor, MI 48109, USA
3. Michigan Psychedelic Center, University of Michigan, Ann Arbor, MI 48109, USA
4. Center for Consciousness Science, University of Michigan, Ann Arbor, MI 48109, USA
5. Neuroscience Graduate Program, University of Michigan, Ann Arbor, MI 48109, USA
6. Department of Chemistry, University of Michigan, Ann Arbor, MI 48109, USA

*****Correspondence: Dinesh Pal, Ph.D.
7433 Medical Science Building 1
1150 West Medical Center Drive
Ann Arbor, Michigan 48109
Ph: 734-615-0234
Email: dineshp@med.umich.edu

Number of pages: 36
Number of figures: 10
Number of tables: 0
Number of words: Abstract: 250
Introduction: 513
Discussion: 1497

Conflict of Interest Statement: The authors declare no competing financial interests.

Acknowledgments: The authors would like to thank Tiecheng Liu, M.D., Christopher Fields, B.S., and Lucy Wang, B.S., for assistance with experiments, and Chris Andrews, Ph.D. (*Consultant, Center for Consulting for Statistics, Computing & Analytics Research, University of Michigan*) for statistical consultation.

Abstract

N,*N*-dimethyltryptamine (DMT) is a serotonergic psychedelic that is being investigated clinically for the treatment of psychiatric disorders. Although the neurophysiological effects of DMT in humans are well-characterized, similar studies in animal models as well as data on the neurochemical effects of DMT are generally lacking, which are critical for mechanistic understanding. In the current study, we combined behavioral analysis, high-density (32-channel) electroencephalography, and ultra-high-performance liquid chromatography-tandem mass spectrometry to simultaneously quantify changes in behavior, cortical neural dynamics, and levels of 17 neurochemicals in medial prefrontal and somatosensory cortices before, during, and after intravenous administration of three different doses of DMT (0.75 mg/kg, 3.75 mg/kg, 7.5 mg/kg) in male and female adult rats. All three doses of DMT produced head twitch response with most twitches observed after the low dose. DMT caused dose-dependent increases in serotonin and dopamine levels in both cortical sites along with a reduction in EEG spectral power in theta (4-10 Hz) and low gamma (25-55 Hz), and increase in power in delta (1-4 Hz), medium gamma (65-115), and high gamma (125-155 Hz) bands. Functional connectivity decreased in the delta band and increased across the gamma bands. In addition, we provide the first measurements of endogenous DMT in these cortical sites at levels comparable to serotonin and dopamine, which together with a previous study in occipital cortex, suggests a physiological role for endogenous DMT. This study represents one of the most comprehensive characterizations of psychedelic drug action in rats and the first to be conducted with DMT.

Significance Statement

N,*N*-dimethyltryptamine (DMT) is a serotonergic psychedelic with potential as a tool for probing the neurobiology of consciousness and as a therapeutic agent for psychiatric disorders. However, the neurochemical and neurophysiological effects of DMT in rat, a preferred animal model for mechanistic studies, are unclear. We demonstrate that intravenous DMT caused a dose-dependent increase in serotonin and dopamine in medial prefrontal and somatosensory cortices, and simultaneously increased gamma functional connectivity. Similar effects have been shown for other serotonergic and atypical psychedelics, suggesting a shared mechanism of drug action. Additionally, we report DMT during normal wakefulness in two spatially and functionally distinct cortical sites — prefrontal, somatosensory — at levels comparable to those of serotonin and dopamine, supporting a physiological role for endogenous DMT.

Introduction

Serotonergic psychedelics, including *N*,*N*-dimethyltryptamine (DMT), produce profound alterations in perception, cognition, mood, and affect in humans (Nichols, 2016) and have been shown to have therapeutic potential for treating a variety of psychiatric disorders (Palhano-Fontes et al., 2019; D'Souza et al., 2022; Goodwin et al., 2022; Holze et al., 2022). DMT has been reported in human blood, urine, and cerebrospinal fluid (Barker et al., 2012) and a recent *in vivo* study revealed the presence of endogenous DMT in occipital cortex, including pineal gland (Dean et al., 2019). However, whether the endogenous DMT is solely restricted to occipital cortex and pineal gland or is present in other cortical areas, is not known. Of note, in contrast to other serotonergic psychedelics, the consciousness-altering effects of DMT are relatively short in duration. When administered intravenously to humans, peak effects occur within approximately three minutes of administration and persist for less than fifteen minutes (Timmermann et al., 2023). The profound and short-acting effects of DMT make it a valuable tool for probing the neurobiology of consciousness, and for future psychedelic-assisted therapies compared to psilocybin or lysergic acid diethylamide (LSD), where dosing sessions can last up to 10 hours (Nichols, 2016). Additionally, the study of endogenous DMT has the potential to provide insights into the mechanisms of action of other serotonergic psychedelics, via an investigation of its properties as a potential neurotransmitter that mediates consciousness or other functions (Vargas et al., 2023).

It has been established that activation of serotonin-2A (5-HT_{2A}) receptors plays a role in mediating the psychoactive effects of DMT (Keiser et al., 2009), but less is known about the neurochemical changes resulting from DMT administration. Early rat studies, in which post-mortem concentrations of neurotransmitters or their metabolites were analyzed after intraperitoneal administration of DMT, showed increases in extracellular dopamine and its primary metabolites

(Haubrich and Wang, 1977; Smith, 1977; Waldmeier and Maître, 1977). Serotonin levels have also been reported to increase in a dose dependent manner following intraperitoneal administration of DMT in rats (Freedman et al., 1970). However, these studies relied on post-mortem analysis of tissue homogenates, lacked spatial resolution, and utilized coarse approaches (e.g., fluorometric analyses), as compared to the more technically sophisticated and robust methodologies in current use (e.g., ultra-high-performance liquid chromatography-tandem mass spectrometry).

Recent human EEG studies using intravenous and inhaled administration of DMT (Timmermann et al., 2019, 2023; Pallavicini et al., 2021) showed a significant reduction in EEG spectral power in alpha and beta bands, along with simultaneous increase in spectral power in delta and gamma range. Additionally, increased corticocortical coherence and signal diversity have also been demonstrated in the gamma range following DMT administration. However, there have been no studies to characterize the effects of DMT administration on neurophysiological dynamics in rodents, which are a valuable translational model for mechanistic studies.

Therefore, in the current study, we determined the effect of intravenous delivery of DMT on changes in 1) behavior, 2) levels of 17 neurochemical analytes including acetylcholine, serotonin, dopamine, γ-aminobutyric acid, and glutamate in prefrontal and somatosensory cortex, and 3) spectral power and functional connectivity across the cortex in rats.

Methods

Rats: The experiments were approved by the Institutional Animal Care and Use Committee at the University of Michigan and were performed in accordance with the Guide for the Care and Use of Laboratory Animals (8th Edition, The National Academies Press), as well as ARRIVE guidelines. Adult male and female Sprague Dawley rats (n = 17, 9 male and 8 female, 300-500g, Charles River

Laboratories) were used for all experiments and were housed in a temperature- and light-controlled facility (12 hours light:12 hours dark cycle, lights on at 8:00 AM), with ad libitum access to food and water.

Surgical procedures: Rats were anesthetized in an induction chamber using 4-5% isoflurane in 100% oxygen. After anesthetic induction, the head was shaved and the rats were immobilized in a stereotaxic frame using blunt ear bars (Model 963, David Kopf Instruments, Tujanga, CA). The rats were positioned to breathe isoflurane through a nose cone (Model 906, David Kopf Instruments, Tujanga, CA), which was titrated to maintain loss of the pedal and palpebral reflex. The delivered isoflurane concentration was monitored throughout the surgical procedure using an anesthetic agent analyzer (Capnomac Ultima, Datex Medical Instrumentation, Tewksbury, MA). Body temperature was maintained at 37°C using a far-infrared heating pad (RT-0502, Kent Scientific, Torrington, CT). Before surgery, subcutaneous buprenorphine (0.01 mg/kg; Buprenex, Par Pharmaceutical, Chestnut Ridge, NY; NDC 42023-179-05) and carprofen (5 mg/kg; Zoetis; NADA #141-199) were administered as presurgical analgesics, and cefazolin (20 mg/kg; West-Ward-Pharmaceutical, Eatontown, NJ; NDC 0143-9924-90) was administered as a prophylactic antibiotic. A sagittal scalp incision was made, and the connective tissue was cleared to expose the skull. Thirty burr holes were drilled across the skull for the implantation of custom-made stainless-steel EEG screw electrodes in a regularly spaced grid of 8 rows that was parallel to coronal suture and spanned the area between 4 mm anterior and 10 mm posterior to bregma; across the 8 rows, the electrodes were arranged in columns parallel and lateral (2 mm to 4.5 mm) to the mid-sagittal suture. Screw electrodes were implanted above the nasal sinus and cerebellum to serve as the reference and ground electrodes, respectively. Two concentric open flow microperfusion (OFM) guide tubes (cOFM-GD-8-2, BASi Research Products, West Lafayette, IN) with dummy inserts

(cOFM-D-10 and cOFM-Lock) were implanted through burr holes aimed at medial prefrontal cortex (mPFC) (from Bregma: 3.0 mm anterior, 0.5 mm mediolateral, and 3.0 mm ventral) and somatosensory barrel field cortex (S1BF) (from Bregma: 3.24 mm posterior, 5.3 mm mediolateral, and 4.0 mm ventral) (Paxinos and Watson, 2007). In addition, all rats were surgically fitted with an indwelling catheter (MRE-040, Micro-Renathane tubing, Braintree Scientific, Braintree, MA) in the jugular vein for intravenous infusion of DMT fumarate (Cayman Chemical, Ann Arbor, MI). All electrodes were secured to a 32-pin Mill-Max connector (Mouser Electronics, Mansfield, TX) and the entire assembly was secured to the cranium with dental cement. Post-surgical buprenorphine (0.03 mg/kg) was administered subcutaneously every 8-12 hours for 48 hours to provide analgesia. The rats were allowed a minimum of 14 days of post-surgical recovery.

Histological Analysis: At the completion of experiments, the rats were euthanized with carbon dioxide inhalation and intracardially perfused with 150 mL of wash solution containing 0.1 M (pH 7.2) phosphate buffered saline (1219SK, EM Sciences, Hatfield, PA) and 1% heparin (1 unitl/mL, Sagent Pharmaceuticals, Schaumburg, IL) followed by 200 mL of a fixative solution containing 4% paraformaldehyde and 4% sucrose in 0.1 M phosphate buffer (pH 7.2). Brains were extracted and stored in the fixative solution for at least 24 hours at 4°C, and then transferred to a 30% sucrose in phosphate buffer solution. Coronal sections (30 µm) were cut through the mPFC and S1BF with a cryostat (Leica Microsystems, Nussloch, Germany). The brain sections were mounted on glass slides and stained with Cresyl violet to confirm the site of OFM probe insertion in mPFC and S1BF regions.

Experimental design: The experimental design is illustrated in figure 1A. The EEG electrode montage and the approximate location of OFM probes is illustrated in figure 1B. The rats were

conditioned to the experimental chambers and EEG recording cables for at least one week before starting the experiments. On the day of the experiment, rats were connected to the EEG recording cable and OFM probes (cOFM-S-10, BASi Research Products, West Lafayette, IN) were lowered into mPFC and S1BF. The probes were connected to a peristaltic microperfusion pump (MPP102 PC, Joanneum Research, Graz, Austria) for continuous perfusion (1 µL/min) with artificial cerebrospinal fluid (aCSF; 145 mM NaCl, Sigma Aldrich S9888; 2.68 mM KCl, Sigma Aldrich P9333; 1.40 mM $CaCl_2$•$2H_2O$, Sigma Aldrich C8106; 1.01 mM $MgSO_4$•$7H_2O$, Sigma Aldrich 63140; 1.55 mM Na_2HPO_4, Sigma Aldrich S5136; 0.45 mM NaH_2PO_4•H2O, Sigma Aldrich 52074; pH 7.4). Data collection began at least one hour after connecting the rats to the EEG cables and OFM probes. EEG and OFM data were collected simultaneously and continuously for the duration of the experiment, which lasted 137.5 minutes. The OFM samples were collected in 12.5 min epochs (1 µL/min) simultaneously from both mPFC and S1BF regions for 11 epochs and consisted of 4 baseline wake epochs (W1-W4) during which rats were freely moving and awake, and 7 drug epochs (D1-D7) after intravenous DMT infusion. The rats were kept awake during the baseline period by gentle tapping on the recording chamber. At the start of the 5th epoch (D1), DMT-fumarate (dissolved in saline) was administered over a 5-minute period (100 µL/min) as an intravenous bolus at one of the following doses: 1) low - 0.75 mg/kg, 2) medium - 3.75 mg/kg, and 3) high - 7.5 mg/kg. A repeated-measures design was utilized in which all rats received each of the three DMT doses in a randomized order with at least 5 days between each dose. Out of the total 51 experimental sessions (17 rats x 3 doses), the mPFC probes failed during 5 experiments and S1BF probes failed during 7 experiments. The EEG data were recorded from all the rats. The OFM samples were collected in a refrigerated fraction collector (4°C) and immediately processed and frozen (-80°C) for ultra-high-performance liquid chromatography-tandem mass spectrometry

(uHPLC-MS/MS) analysis. All experiments were video recorded for later behavioral analysis by an investigator blinded to the experimental condition. At the conclusion of data collection, the OFM sample collection sites were histologically verified (Fig. 1C-D).

Behavioral analysis: All experiments were video recorded. The details of the experimental sessions were masked to allow for blinded analysis. General behavioral patterns were observed and documented for the duration of each experiment. Head-twitch response (HTR), defined as a rapid, side-to-side rotational movement of the head independent of grooming behavior, was quantified during a 15-minute window, starting at the beginning of the DMT infusion (D1).

Neurochemical quantification via ultra-high-performance liquid chromatography-tandem mass spectrometry (uHPLC-MS/MS): To prepare perfusate samples for uHPLC-MS/MS analysis, 10 µL of sample was mixed with 2.5 µL of carbonate buffer (200 mM), and derivatized with 25 µL of 2% benzoyl chloride (Sigma Aldrich 259950) in acetonitrile (v/v), and the mixture was centrifuged for 10 minutes to precipitate proteins. To normalize for extraction efficiency and mass spectrometry ionization efficiency, 9 µL of the supernatant was spiked with 11 µL of internal standard, which contained ^{13}C- or deuterium-labeled derivatives of all analytes of interest (see **extended data table 1-1** for a list of analytes and multiple reaction monitoring scanning parameters). Prior to each uHPLC-MS/MS analysis, 6-point calibration curves were constructed for each analyte based on the peak area ratio of the calibration standard to the internal standard by linear regression. Calibration standards consisted of a mixture of all compounds of interest and were spiked with the corresponding ^{13}C- or deuterium-labeled internal standard. All samples and standards were analyzed using a Phenomenex Kinetex C18 chromatography column (100 x 2.1 mm, 1.7 µm, 100 Å) on a Vanquish uHPLC (Thermo Fisher Scientific, Gemering, Germany) interfaced to a TSQ Quantum Ultra triple quadrupole mass spectrometer (Thermo Fisher Scientific,

San Jose, CA). Mobile phase A was 10 mM ammonium formate with 0.15% (v/v) formic acid in water. Mobile phase B was acetonitrile. The gradient used was as follows: initial, 5% B; 0.01 min, 19% B; 0.68 min, 26% B; 1.05 min, 75% B; 1.8 min, 100% B; 2.2 min, 100% B; 2.3 min, 5% B; 3.0 min, 5% B. The flow rate was maintained at 600 μL/min and the sample injection volume was 7.5 μL. The autosampler was kept at ambient temperature, with the column being held at 30°C in still air mode. Electrospray ionization was used in positive mode at 4 kV. The capillary temperature was 325°C, the vaporizer temperature was 300°C, the sheath gas pressure was 50 Arb, and the auxiliary gas pressure was 10 Arb. Ions were detected in tandem mass spectrometry mode. Automatic peak integration was performed using XCalibur 3.0 MS software, and all peaks were visually inspected to ensure accurate integration. The following 17 analytes were included in neurochemical analyses: acetylcholine, adenosine, aspartate, choline, dopamine, DMT, GABA, glucose, glutamate, glutamine, glycine, histamine, homovanillic acid, phenylalanine, serine, serotonin, and taurine.

EEG data acquisition and analysis: Monopolar EEG data were acquired using a 32-channel head stage (Cereplex μ, Blackrock Microsystems, Salt Lake City, UT). The signals were digitized at 1 kHz and bandpass filtered between 0.1-500 Hz using a Cereplex Direct system paired with the Cereplex Direct Software Suite (Blackrock Microsystems, Salt Lake City, UT). Raw EEG signals were imported into MATLAB (version 2022b; MathWorks, Inc.; Natick, MA) and data segments with movement or hardware artifacts were removed after identification by visual inspection of both the raw waveform and spectrogram of the EEG signals in 10-second windows. EEG segments containing slow-waves, indicative of sleep or a sleep-like state, were excluded. Bad channels were also visually identified and excluded. Segments of clean EEG data (total lengths between 1 and 5 minutes per epoch) were subsequently used to compute power spectrum density (PSD) and

weighted phase lag index (wPLI) within each of the following frequency bands: delta (1-4 Hz), theta (4-10 Hz), low gamma (25-55 Hz), medium gamma (65-115 Hz), and high gamma (125-155 Hz). PSD was calculated using Matlab's implementation of Welch's method (pwelch.m) at the channel-level on clean data segments (10-second moving window, 90% overlap, 2-second Hamming window) and then averaged across all channels. Relative power was calculated as the absolute power within a given frequency divided by the total absolute power across all frequencies for each of the 11 epochs. wPLI is a measure of functional connectivity based on the phase relationship between two signals and is robust to volume conduction (Vinck et al., 2011). Before computing wPLI, the full continuous data recordings were bandpass filtered to the desired frequency band using FieldTrip's implementation of a windowed-sinc finite impulse response filter (Oostenveld et al., 2010). Artifact-free segments (between 1 and 5 minutes) of the filtered EEG data — identical to those used for PSD — were extracted for analysis. A Hilbert transform was used to extract the analytic signal from each electrode. The complex conjugate of each channel pair ($\boldsymbol{xy}$) was subsequently used to estimate the cross spectrum ($\boldsymbol{C_{xy}}$), with the imaginary component of the cross spectrum being $\boldsymbol{\Im_{xy}}$. wPLI was then estimated for 10-second non-overlapping windows using the following equation:

$$wPLI_{xy} = \frac{\left|E\{\Im_{xy}\}\right|}{E\{\left|\Im_{xy}\right|\}}$$

wPLI values were subsequently normalized using surrogate data (n = 50) generated through phase-shuffling while preserving the amplitude distribution of each signal. The normalized wPLI ($wPLI_{norm}$) was then computed using the mean (μ_{shuff}) and standard deviation (σ_{shuff}) of the surrogate data:

$$wPLI_{norm} = \frac{wPLI_{raw} - \mu_{shuff}}{\sigma_{shuff}}$$

Global wPLI was computed by averaging across all channel pairs for each frequency band for each of the 11 epochs.

Statistical analysis: All statistical analyses were completed with R software (RStudio version 2023.09.1+494). The sample size (n=17 rats) was decided based on a priori power analyses conducted using neurochemical and neurophysiological pilot data from DMT studies in our lab and was informed by the neurochemical data (changes in acetylcholine) from a previous publication (Brito et al., 2021). Primary outcome measures included DMT-induced HTR, changes in the levels of neurotransmitters, and the changes in EEG measures of relative spectral power and functional connectivity (wPLI). For analysis of HTR data, a linear mixed model was implemented, with 'dose' treated as a fixed factor and 'subject' treated as a random intercept. An alpha threshold of $p<0.05$ was utilized and the Tukey method was used for p value adjustment of estimated contrasts between each dose. Raw concentrations of each of the neurochemical analytes were log (base 10) transformed. For each experiment, the 11 samples collected from each rat at each of the three doses were grouped into 4 epochs, identified as 'wake' (W1-W4), 'drug' (D1-D2), 'post-drug' (D3-D5), and 'recovery' (D6-D7) and averaged accordingly. A linear mixed model was implemented in which 'dose' and 'state' were treated as fixed factors and 'subject' was treated as a random intercept to account for intersubject variability. Separately for each dose, the model was used to compare the 'drug,' 'post-drug,' and 'recovery' epochs with the baseline 'wake' epoch. To generate plots for neurochemical data, the 'wake' epoch was normalized to zero and changes relative to 'wake' were plotted for the 'drug,' 'post-drug,' and 'recovery' epochs. Mean values are shown for each dose with error bars indicating standard error of the mean (s.e.m.), unless noted otherwise. To assess the relationship between the levels of DMT, serotonin, and dopamine in the brain after DMT administration, Spearman's rank correlation was used. Correlation coefficients

(ρ) were calculated for each dose, and two-tailed t-tests with an alpha threshold of $p<0.05$ were conducted to test for statistical significance. For EEG analysis, a similar model was implemented, but each of the 7 drug epochs (D1-D7) were compared to the averaged baseline 'wake' epoch. For neurochemical and EEG data, an alpha threshold of $p<0.05$ was utilized, and p values were adjusted for multiple comparisons via Dunnett's test. Estimated contrasts between each state, as well as the percent change from baseline, t statistics, 95% confidence intervals (CI) and p values are reported for each comparison throughout the results section.

Results

Histological analysis confirmed the location of OFM probes to be within mPFC (**Fig. 1C**) and S1BF (**Fig. 1D**).

Effect of intravenous DMT administration on behavior: The onset of behavioral effects typically began within 1 minute after the start of DMT infusion. The duration of behavioral changes showed a dose-dependent pattern with the effects lasting approximately 10-20 minutes after the low dose, 20-30 minutes after the medium dose, and 30-40 minutes after the high dose. For all doses, behavioral arousal was the first observed effect and occurred within the first 1-2 minutes after the start of the DMT infusion, and typically included exploratory behaviors such as rearing and sniffing. The majority of head twitches occurred during the 5-minute period immediately after the infusion of DMT. Average number of head twitches (±s.e.m.) during the 15-minute period starting at the beginning of the DMT infusions were: 6.6 ± 6.0 (low dose), 2.9 ± 2.1 (medium dose), and 2.6 ± 2.4 (high dose). The low dose caused significantly more head twitches when compared to the medium dose ($t[31]=3.6$, CI=0.34-6.78, $p<0.05$) and high dose ($t[31]=4.0$, CI=0.92-7.14,

$p<0.01$) (**Fig. 2A)**. Following the period of behavioral arousal and head twitches at the low dose, rats typically showed 10-20 minutes of inactivity and flattened body posture, with normal behavior returning approximately 30 minutes after the end of the infusion. During the 5-10 minute period after DMT infusion, the medium and high doses resulted in behaviors associated with serotonin syndrome, such as hind limb abduction and head weaving. The high dose showed the most pronounced manifestation of serotonin syndrome, which included all behaviors previously mentioned along with occasional forepaw treading, Straub tail, and backward walking. A period of inactivity followed these behaviors, which lasted for 20-30 minutes after the medium dose and 30-40 minutes following the high dose, after which the behavioral patterns returned to that observed during baseline wake state. There were no behavioral differences between males and females at any dose (**Fig. 2B**).

Effect of intravenous administration of DMT on cortical DMT concentration: DMT concentrations in mPFC and S1BF increased in a dose-dependent manner immediately after intravenous infusion of DMT (i.e. during the D1 epoch) (**Fig. 3**). The peak concentration (nM) in mPFC were (mean ± s.e.m.): 39.96 ± 7.76 for the low dose, 236.08 ± 60.03 for the medium dose, and 830.17 ± 405.09 for the high dose. The peak concentrations (nM) in S1BF were (mean ± s.e.m.): 38.14 ± 9.06 for the low dose, 183.11 ± 48.61 for the medium dose, and 369.70 ± 120.79 for the high dose. After the low-dose DMT infusion, the levels of DMT in mPFC (**Fig. 3A**) and S1BF (**Fig. 3B**) remained elevated until approximately 50 minutes after the start of DMT infusion (i.e., the D4 epoch). For the medium and high doses, the levels of DMT in both brain regions remained significantly higher than the baseline levels throughout the duration of the experiment (i.e., 87.5 minutes after the start of DMT infusion) (**Fig. 3A-B**). The levels of DMT detected in mPFC and S1BF after intravenous infusion peaked during the D1 and D2 epochs and then

gradually declined towards baseline. Therefore, to align the neurochemical analyses with the peak concentrations of DMT in the brain, we grouped the data into four states: wake (W1-W4), drug (D1-D2), post-drug (D3-D5), and recovery (D6-D7) (**Fig. 3C-D**).

Effect of intravenous administration of DMT on cortical neurochemistry: Intravenous DMT administration resulted in dose-dependent changes in the levels of 5-HT and dopamine in both mPFC and S1BF (**Fig. 4**). As compared to the baseline wake state, intravenous administration of DMT at the medium and high doses caused a significant increase in 5-HT during the drug epoch in mPFC (medium dose: 221%, $t[109]=5.73$, $p<0.001$; high dose: 302%, $t[109]=7.98$, $p<0.001$) and S1BF (medium dose: 165%, $t[116]=3.39$, $p<0.001$; high dose: 184%, $t[116]=3.85$, $p<0.001$) (**Fig. 4A-B**). The low dose of DMT did not produce any statistically significant effect on 5-HT levels during the Drug epoch but did cause a significant decrease in 5-HT concentration during the recovery period in both brain regions (mPFC: -66%, $t[110]=-3.11$, $p<0.001$; S1BF: -66%, $t[117]=-2.42$, $p=0.01$) (**Fig. 4A-B**). Dopamine levels were affected only by the high dose of DMT, which showed a significant increase during the drug epoch in mPFC (178%, $t[137]=4.51$, $p<0.001$) and S1BF (146%, $t[80]=2.77$, $p<0.05$) (**Fig. 4C-D**). Apart from 5-HT and dopamine, we did not find any statistically significant changes during the drug epoch for the rest of the analytes but did observe changes during the post-drug and recovery epochs (**Fig. 5**). In mPFC, a significant decrease during both the post-drug and recovery epochs were observed for glycine (post-drug: -78%, $t[153]=-.59$, $p<0.05$; recovery: -78%, $t[153]=-2.52$, $p<0.05$), phenylalanine (post-drug: -79%, $t[150]=-2.59$, $p<0.05$; recovery: -77%, $t[150]=-2.79$, $p<0.05$), and taurine (post-drug: -81%, $t[150]=-2.52$, $p<0.05$; recovery: -80%, $t[150]=-2.68$, $p<0.05$); the decrease was observed only after administration of the high dose. The neurochemical changes in S1BF were as follows: low dose DMT resulted in a significant decrease during the recovery epoch in levels of glucose (-77%,

t[141]=-3.22, p<0.01) and taurine (-85%, t[145]=-2.49, p<0.05). At the high dose, a significant decrease was observed during the recovery epoch in levels of adenosine (-76%, t[140]=-2.67, p<0.05) and glucose (-77%, t[141]=-3.10, p<0.01). The high dose also resulted in a significant decrease in levels of the following analytes during both the post-drug and recovery epochs: glycine (post-drug: -81%, t[145]=-3.33, p<0.01; recovery: -80%, t[145]=-3.55, p<0.01), phenylalanine (post-drug: -83%, t[141]=-3.12, p<0.01; recovery: -83%, t[141]=-3.0, p<0.01), and serine (post drug: -86%, t[145]=-2.43, p<0.05; Recovery:-85%, t145]=-2.58, p<0.05). Lastly, taurine levels were significantly reduced (-85%, t[145]=-2.49, p<0.05) during the post-drug epoch after the administration of high dose DMT. Basal concentrations of the 17 analytes from both mPFC and S1BF are provided in **extended Table 5-1**.

Because the most salient neurochemical change following DMT administration was the increase in 5-HT and dopamine levels, we next assessed the relationship between the levels of 5-HT and dopamine and the associated levels of recoverable DMT in both brain regions during the D1-D7 epochs. Spearman correlation coefficients were computed using log transformed values of 5-HT, dopamine, and DMT in both mPFC and S1BF for each of the three doses. These analyses revealed significant positive correlation between 5-HT and recoverable DMT concentration as well as dopamine and recoverable DMT concentration, in both brain regions (**Fig. 6**). These correlations were largely dose-dependent, where the highest dose showed the strongest correlation for 5-HT in S1BF and for dopamine in both brain regions.

Endogenous DMT was detected during baseline wake condition in 70% of the mPFC experiments and 80% of the S1BF experiments. The mean (± s.e.m.) DMT concentration was 0.66 ± 0.08 nM

in mPFC and 0.54 ± 0.11 nM in S1BF, which was similar to that observed for 5-HT and dopamine in these brain regions (**Fig. 7**).

Effect of intravenous administration of DMT on EEG spectral power: In addition to analyzing neurochemical changes in mPFC and S1BF, we simultaneously also conducted continuous high-density EEG recording to determine the effect of intravenous DMT on cortical neural dynamics. Statistically significant changes in EEG spectral power were observed after DMT infusions at each of the three doses (**Fig. 8**). As compared to the baseline wake epoch, DMT infusion (i.e., D1 epoch) was characterized by a global increase in spectral power in delta band (low dose: 177%, $t[519]=6.26$, $p<0.001$; medium dose: 135%, $t[519]=4.78$, $p<0.001$) (**Fig. 8A**), medium gamma band (medium dose: ~1%, $t[519]=7.89$, $p<0.001$; high dose: ~1%, $t[519]=5.18$, $p<0.001$) (**Fig. 8D**), and high gamma band (low dose: ~1%, $t[519]=2.68$, $p<0.05$; medium dose: ~1%, $t[519]=7.89$, $p<0.001$; high dose: ~1%, $t[519]=4.74$, $p<0.001$) (**Fig. 8E**). Simultaneously, there was a significant decrease in spectral power in theta band (low dose: -109%, $t[519]=-8.07$, $p<0.001$; medium dose: -100%, $t[519]=-7.45$, $p<0.001$) (**Fig. 8B**), and low gamma band (high dose: 1.1%, $t[519]=-2.99$, $p<0.05$) (**Fig. 8C**). Statistically significant changes were also observed during the D2-D7 epochs in delta, theta, and gamma bands at all three doses. The high dose DMT produced increase in delta power in D2 epoch, which remained elevated for the rest of the recording period, with statistically significant increase in D3 and D5 epochs. After the initial decrease in D1 epoch, the low gamma power showed a generalized increase at all doses for the rest of the recording period. Similarly, high dose DMT showed a delayed effect on theta power, which decreased significantly in D2 epoch, and then remained significantly low during the entire recoding period. See **extended data tables 8-1, 8-2, and 8-3** for a summary of statistical comparisons of EEG power spectral changes.

Effect of intravenous administration of DMT on functional connectivity: As compared to the baseline wake state, global delta connectivity was significantly reduced during the D1 epoch for the low dose (-15,4%, t[519]=-6.41, p<0.001) and medium dose (-9.7%, t[519]=-4.06, p<0.001) (**Fig. 9A**). This effect appeared after a delay for the high dose and occurred during the D2 epoch (-16.8%, t[519]=-6.98, p<0.01). The high dose DMT also resulted in a significant increase in theta connectivity during the D1 epoch (5.7%, t[519]=5.96, p<0.001), followed by a significant decrease in theta connectivity during the D2 epoch (-3.7%, t[519]=-3.85, p=0.001) (**Fig. 9B**). Finally, all three doses produced significant increase in connectivity during the D1 epoch across all three gamma bands: Low gamma band (low dose: 2.1%, t[519]=7.48, p<0.001; medium dose: 1.6%, t[519]=5.68, p<0.001; high dose: 4.9%, t[519]=9.19, p<0.001) (**Fig. 10A**), Medium gamma band (low dose: 1.0%, t[508]=3.55, p<0.01; medium dose: 1.7%, t[508]=5.88, p<0.001; high dose: 1.7%, t[508]=6.37, p<0.001) (**Fig. 10B**), and High gamma band (low dose: 3.3%, t[519]=6.25, p<0.001; medium dose: 5.9%, t[519]=11.02, p<0.001; high dose: 4.9%, t[519]=9.19, p<0.001) bands (**Fig. 10C**). A significant increase in global gamma connectivity persisted for both the medium and high doses and returned to baseline levels in a dose-dependent manner. See **extended data tables 9-1, 9-2 and 9-3** for a summary of statistical comparisons of global connectivity changes.

Of note, the global decrease in delta connectivity appears to be driven by frontal-parietal and frontal-occipital electrode pairs (**Fig. 9A**) whereas the changes in global theta connectivity originated predominantly from parietal-occipital electrode pairs (**Fig. 9B**). The increase in low gamma connectivity also appears to be driven by parietal-occipital electrode pairs (**Fig. 10A**), whereas increase in medium gamma connectivity appears to be primarily driven by frontal-parietal

electrode pairs (**Fig. 10B**). The changes in the high gamma connectivity (**Fig. 10C**) were primarily driven by the frontal electrode pairs.

Discussion

In this study, we report that intravenous DMT caused a dose-dependent increase in 5-HT and dopamine in mPFC and S1BF, and produced head twitches — a behavioral surrogate for psychedelic drug action in rodents — which decreased with increasing doses. The most salient EEG changes were increase in spectral power and functional connectivity in the gamma bandwidth. Notably, we present the first report of endogenous DMT during normal wakefulness in prefrontal and somatosensory cortices at levels consistent with conventional neurotransmitters.

Subcutaneous or intraperitoneal administration of DMT in rodents (Corne and Pickering, 1967; Stoff et al., 1978; Geyer et al., 1979; Jenner et al., 1980; Commissaris and Davis, 1983; González-Maeso et al., 2007; Cameron et al., 2018) has been reported to produce head twitches, hind limb abduction, low body posture and tremors, Straub tail, forepaw treading, and head weaving (Jenner et al., 1980). Our results are consistent with these previous findings and in addition demonstrated the dose-dependency of behavioral phenotypes. The incidence of head twitches was significantly higher following the low dose compared to medium or high doses. This pattern has been reported previously with DMT and other phenylalkylamine and tryptamine hallucinogens, where a substantial decrease in HTR occurs at higher doses (Fantegrossi et al., 2006, 2008; Halberstadt et al., 2020). This biphasic phenomenon has been hypothesized to be mediated by differential receptor activation, with 5-HT_{2A} receptor activation driving the ascending portion of the HTR curve and 5-HT_{2C} receptor activation driving the descending portion (Fantegrossi et al., 2010).

Our rigorous technical approach to assessing neurochemical dynamics allowed for quantification of endogenous DMT during baseline normal wake condition in freely behaving rats, something that had only been done in a previous study of occipital cortex (Dean et al., 2019). We demonstrated that the levels of DMT in mPFC and S1BF during normal wakefulness are within the ranges of both 5-HT and dopamine, suggesting a physiological role for endogenous DMT, and supporting further investigation of DMT as a possible neurotransmitter. After intravenous administration, peak DMT levels in both cortical sites persisted for approximately 25 minutes and remained significantly elevated above baseline for more than 90 minutes for medium and high doses. This contrasts with the reported metabolic course of DMT in plasma after intravenous administration of hallucinogenic doses in humans; DMT concentrations peak at approximately 2 minutes and quickly decrease toward basal levels within 20 minutes (Timmermann et al., 2019). In rats, levels of recoverable DMT have been shown to be more than 5-fold higher in brain tissues as compared to that in blood, for up to 60 minutes after administration (Takahashi et al., 1985; Sitaram et al., 1987). These previous findings and the results of this study suggest a potential storage or sequestration mechanism for DMT in the brain (Cozzi et al., 2009), or differential enzymatic clearance mechanisms between blood and brain tissues.

We found positive correlations between levels of recoverable DMT and levels of 5-HT and dopamine in mPFC and S1BF. Given the established role of 5-HT and dopamine in mediating mood and affect, these dose-dependent linear relationships suggest that DMT induced an altered state in rats, likely via an increase in endogenous neurotransmitters. Previous studies have shown that DMT acts as a 5-HT releaser, and has affinity at serotonin and dopamine transporters, which would presumably inhibit reuptake of the respective neurotransmitters, and cause increase in extracellular concentrations (Cozzi et al., 2009; Blough et al., 2014; Rickli et al., 2016).

Additionally, DMT is not only a substrate, but also an inhibitor of monoamine oxidase (Ho et al., 1970; Ungar and Alivisatos, 1976; Barker et al., 1980), the primary enzyme responsible for metabolism of 5-HT and dopamine. Thus, sufficiently high concentrations of DMT may competitively inhibit monoamine oxidases, resulting in reduced metabolism of other endogenous monoamines. It has also been established that activation of 5-HT_{2A} receptors can directly regulate 5-HT levels in prefrontal cortex by increasing firing of dorsal raphe 5-HT neurons (Martín-Ruiz et al., 2001) and dopamine levels through a feedback pathway involving efferent projections to the ventral tegmental area (Pehek et al., 2006; Alex and Pehek, 2007). We observed a significant decrease in phenylalanine — an essential amino acid precursor of tyrosine and hence catecholamine synthesis — in the post-drug and recovery period in both brain regions, which may indicate increased phenylalanine uptake into neurons to replenish depleted dopamine stores. Of note, a recent study (Wojtas et al., 2022) reported increase in 5-HT and dopamine levels in frontal cortex of rat after intraperitoneal administration of psilocybin and ketamine, which along with the results from the current study, suggests a shared mechanism of action of psychedelic drugs.

We also quantified the levels of several other neurotransmitters and signaling molecules, none of which showed a significant change during the acute drug state when DMT concentrations peaked in the brain. Of particular interest is the absence of a change in glutamate levels. This is unexpected considering the well-established finding that 5-HT_{2A} receptor activation causes increased glutamatergic excitatory postsynaptic currents in the mPFC, which is a region with high density of 5-HT_{2A} receptors (Aghajanian and Marek, 1999; Béïque et al., 2007). Accordingly, serotonergic psychedelics including LSD, psilocybin, and the 5-HT_{2A} agonist 2,5-dimethoxy-4-iodoamphetamine (DOI) have been reported to increase extracellular glutamate in the mPFC (Scruggs et al., 2003; Muschamp et al., 2004; Wojtas et al., 2022). Increased glutamatergic

neurotransmission in layer V pyramidal neurons of the mPFC has been proposed as a key mechanism of psychedelic action and their neuroplasticity-promoting effects (Vollenweider and Kometer, 2010; Vollenweider and Preller, 2020). Although direct evidence for increased glutamate release in mPFC exists for other serotonergic psychedelics, this had previously not been established for DMT.

EEG results revealed persistent decreases in theta power at all three doses. This has been reported previously in human studies with psilocybin, LSD, and the atypical psychedelic, ketamine (Muthukumaraswamy et al., 2013; Pallavicini et al., 2019; Barnett et al., 2020). Previous human studies with DMT have also reported a reduction in alpha power as a neurophysiological correlate of DMT (Timmermann et al., 2019, 2023; Pallavicini et al., 2021). In contrast to humans where alpha oscillations are dominant, theta oscillations dominate in rats (Klimesch, 1999). Theta oscillations, which are generated in the hippocampus (Buzsáki, 2002), have long been associated with voluntary movement in rodents (Vanderwolf, 1969), but also play a major role in the synchronization of activity between hippocampal and cortical regions, which is required for learning, memory, and cognitive tasks (Zangbar et al., 2020). Thus, these results align with previous investigations and may be associated with disrupted communication between hippocampal and cortical regions following DMT.

Functional connectivity analyses revealed a pattern in which delta and theta connectivity diminished, giving way to increased gamma connectivity following DMT. For low and medium gamma frequencies, connectivity increases were observed primarily in electrode pairs involving parietal and occipital regions, whereas frontal electrode pairs were the primary contributors to the increased connectivity after the high gamma range. The duration and intensity of gamma changes were dose-dependent, with the highest dose causing the longest and most pronounced changes.

Similar findings were reported in a recent rat study that demonstrated hypersynchronous high frequency gamma oscillations after serotonergic (LSD, DOI) and atypical psychedelics (ketamine) (Brys et al., 2023). In humans, changes in low gamma oscillations resulting from DMT (Pallavicini et al., 2021) and psilocybin (Kometer et al., 2015) correlate with several aspects of the subjective experience. Gamma rhythms represent fundamental components of cortical computation (Fries, 2009; Sohal et al., 2009) and are thought to play a major role in effective corticocortical connectivity (Fries, 2015). Therefore, such alterations in gamma oscillations may underlie the non-ordinary states of consciousness induced by psychedelic drugs.

Of note, to improve experimental rigor and translational applicability, we employed intravenous infusions of DMT, which allowed controlled and precise drug delivery into systemic circulation. In addition, we used OFM for neurochemical sampling, which offers two distinct advantages compared to conventional neurochemical sampling with microdialysis probes. First, unlike microdialysis probes, OFM probes do not extend beyond the guide tubes, thereby preventing damage to the blood-brain barrier and surrounding brain tissue, which eliminates potential confounds associated with inflammation and tissue scarring. Second, OFM probes do not use a semi-permeable membrane, which improves analyte recovery.

A limitation of our study is that the low temporal resolution of OFM sampling prevented assessment of transient or phasic neurochemical dynamics, potentially masking acute neurochemical changes. Furthermore, we did not investigate the effects of other psychedelic agents, which could have allowed a direct comparison to the current data. Despite these limitations, this study represents one of the most comprehensive neurochemical characterization of psychedelic drug action in rodents to date, and the neurophysiological changes mapped by functional connectivity suggests translational relevance of rodent models in investigating the

neurobiology of DMT. Lastly, for the first time we demonstrated that DMT is present in prefrontal and somatosensory cortices of freely behaving normally behaving and awake rats at levels within the range of 5-HT and dopamine, a finding that motivates future investigation into the physiological role of DMT as a putative neurotransmitter.

References

Aghajanian GK, Marek GJ (1999) Serotonin, via 5-HT2A receptors, increases EPSCs in layer V pyramidal cells of prefrontal cortex by an asynchronous mode of glutamate release. Brain Res 825:161–171.

Alex KD, Pehek EA (2007) Pharmacologic mechanisms of serotonergic regulation of dopamine neurotransmission. Pharmacol Ther 113:296–320.

Barker SA, Borjigin J, Lomnicka I, Strassman R (2013) LC/MS/MS analysis of the endogenous dimethyltryptamine hallucinogens, their precursors, and major metabolites in rat pineal gland microdialysate. Biomed Chromatogr 27:1690–1700.

Barker SA, McIlhenny EH, Strassman R (2012) A critical review of reports of endogenous psychedelic N, N-dimethyltryptamines in humans: 1955–2010. Drug Test Anal 4:617–635.

Barker SA, Monti JA, Christian ST (1980) Metabolism of the hallucinogen N,N-dimethyltryptamine in rat brain homogenates. Biochem Pharmacol 29:1049–1057.

Barnett L, Muthukumaraswamy SD, Carhart-Harris RL, Seth AK (2020) Decreased directed functional connectivity in the psychedelic state. Neuroimage 209:116462.

Blough BE, Landavazo A, Decker AM, Partilla JS, Baumann MH, Rothman RB (2014) Interaction of psychoactive tryptamines with biogenic amine transporters and serotonin receptor subtypes. Psychopharmacology 231:4135–4144.

Brito MA, Li D, Fields CW, Rybicki-Kler C, Dean JG, Liu T, Mashour GA, Pal D (2021) Cortical Acetylcholine Levels Correlate With Neurophysiologic Complexity During Subanesthetic Ketamine and Nitrous Oxide Exposure in Rats. Anesth Analg 134:1126-1139.

Brys I, Barrientos SA, Ward JE, Wallander J, Petersson P, Halje P (2023) 5-HT2AR and NMDAR psychedelics induce similar hyper-synchronous states in the rat cognitive-limbic cortex-basal ganglia system. Commun Biol 6:737.

Buzsáki G (2002) Theta Oscillations in the Hippocampus. Neuron 33:325–340.

Cameron LP, Benson CJ, Dunlap LE, Olson DE (2018) Effects of N, N-Dimethyltryptamine on Rat Behaviors Relevant to Anxiety and Depression. ACS Chem Neurosci 9:1582–1590.

Commissaris RL, Davis M (1983) Opposite effects of N,N-dimethyltryptamine (DMT) and 5-methoxy-N,N-dimethyltryptamine (5-MeODMT) on acoustic startle: Spinal vs brain sites of action. Neurosci Biobehav Rev 6:515–520.

Corne SJ, Pickering RW (1967) A possible correlation between drug-induced hallucinations in man and a behavioural response in mice. Psychopharmacologia 11:65–78.

Cozzi NV, Gopalakrishnan A, Anderson LL, Feih JT, Shulgin AT, Daley PF, Ruoho AE (2009) Dimethyltryptamine and other hallucinogenic tryptamines exhibit substrate behavior at the serotonin uptake transporter and the vesicle monoamine transporter. J Neural Transm 116:1591.

Dean JG, Liu T, Huff S, Sheler B, Barker SA, Strassman RJ, Wang MM, Borjigin J (2019) Biosynthesis and Extracellular Concentrations of N,N-dimethyltryptamine (DMT) in Mammalian Brain. Sci Rep 9:9333.

D'Souza DC, Syed SA, Flynn LT, Safi-Aghdam H, Cozzi NV, Ranganathan M (2022) Exploratory study of the dose-related safety, tolerability, and efficacy of dimethyltryptamine (DMT) in healthy volunteers and major depressive disorder. Neuropsychopharmacology 47:1854–1862.

Fantegrossi WE, Harrington AW, Kiessel CL, Eckler JR, Rabin RA, Winter JC, Coop A, Rice KC, Woods JH (2006) Hallucinogen-like actions of 5-methoxy-N,N-diisopropyltryptamine in mice and rats. Pharmacol Biochem Be 83:122–129.

Fantegrossi WE, Reissig CJ, Katz EB, Yarosh HL, Rice KC, Winter JC (2008) Hallucinogen-like effects of N,N-dipropyltryptamine (DPT): Possible mediation by serotonin 5-HT1A and 5-HT2A receptors in rodents. Pharmacol Biochem Behav 88:358–365.

Fantegrossi WE, Simoneau J, Cohen MS, Zimmerman SM, Henson CM, Rice KC, Woods JH (2010) Interaction of 5-HT2A and 5-HT2C Receptors in R(−)-2,5-Dimethoxy-4-iodoamphetamine-Elicited Head Twitch Behavior in Mice. J Pharmacol Exp Ther 335:728–734.

Freedman DX, Gottlieb R, Lovell RA (1970) Psychotomimetic drugs and brain 5-hydroxytryptamine metabolism. Biochem Pharmacol 19:1181–1188.

Fries P (2009) Neuronal Gamma-Band Synchronization as a Fundamental Process in Cortical Computation. Annu Rev Neurosci 32:209–224.

Fries P (2015) Rhythms for Cognition: Communication through Coherence. Neuron 88:220–235.

Geyer MA, Light RK, Rose GJ, Petersen LR, Horwitt DD, Adams LM, Hawkins RL (1979) A characteristic effect of hallucinogens on investigatory responding in rats. Psychopharmacology 65:35–40.

González-Maeso J, Weisstaub NV, Zhou M, Chan P, Ivic L, Ang R, Lira A, Bradley-Moore M, Ge Y, Zhou Q, Sealfon SC, Gingrich JA (2007) Hallucinogens Recruit Specific Cortical 5-HT2A Receptor-Mediated Signaling Pathways to Affect Behavior. Neuron 53:439–452.

Goodwin GM et al. (2022) Single-Dose Psilocybin for a Treatment-Resistant Episode of Major Depression. New Engl J Med 387:1637–1648.

Goodwin GM, Green AR (1985) A behavioural and biochemical study in mice and rats of putative selective agonists and antagonists for 5-HT1 and 5-HT2 receptors. Brit J Pharmacol 84:743–753.

Goodwin GM, Souza RJD, Green AR, Heal DJ (1987) The pharmacology of the behavioral and hypothermic responses of rats to 8-hydroxy-2-(di-n-propylamino)tetralin (8-OH-DPAT). Psychopharmacology 91:506–511.

Halberstadt AL, Chatha M, Klein AK, Wallach J, Brandt SD (2020) Correlation between the potency of hallucinogens in the mouse head-twitch response assay and their behavioral and subjective effects in other species. Neuropharmacology 167:107933.

Halberstadt AL, Geyer MA (2013) Characterization of the head-twitch response induced by hallucinogens in mice. Psychopharmacology 227:727–739.

Haubrich DR, Wang PFL (1977) N,N-dimethyltryptamine lowers rat brain acetylcholine and dopamine. Brain Res 131:158–161.

Ho BT, McIsaac WM, An R, Harris RT, Walker KE, Kralik PM, Airaksinen MM (1970) Biological activities of some 5-substituted N,N-dimethyltryptamines, α-methyltryptamines, and gramines. Psychopharmacologia 16:385–394.

Holze F, Gasser P, Müller F, Dolder PC, Liechti ME (2022) Lysergic acid diethylamide-assisted therapy in patients with anxiety with and without a life-threatening illness A randomized, double-blind, placebo-controlled Phase II study. Biol Psychiatry.

Isbister GK, Buckley NA (2005) The Pathophysiology of Serotonin Toxicity in Animals and Humans. Clin Neuropharmacol 28:205–214.

Jenner P, Marsden CD, Thanki CM (1980) Behavioural changes induced by N,N-dimethyl-tryptamine in rodents. Br J Pharmacol 69:69–80.

Keiser MJ, Setola V, Irwin JJ, Laggner C, Abbas A, Hufeisen SJ, Jensen NH, Kuijer MB, Matos RC, Tran TB, Whaley R, Glennon RA, Hert J, Thomas KLH, Edwards DD, Shoichet BK, Roth BL (2009) Predicting new molecular targets for known drugs. Nature 462:175–181.

Klimesch W (1999) EEG alpha and theta oscillations reflect cognitive and memory performance: a review and analysis. Brain Res Rev 29:169–195.

Kometer M, Pokorny T, Seifritz E, Volleinweider FX (2015) Psilocybin-induced spiritual experiences and insightfulness are associated with synchronization of neuronal oscillations. Psychopharmacology 232:3663–3676.

Lu J-Q, Nagayama H (1996) Circadian rhythm in the response of central 5-HT1A receptors to 8-OH-DPAT in rats. Psychopharmacology 123:42–45.

Martín-Ruiz R, Puig MV, Celada P, Shapiro DA, Roth BL, Mengod G, Artigas F (2001) Control of Serotonergic Function in Medial Prefrontal Cortex by Serotonin-2A Receptors through a Glutamate-Dependent Mechanism. J Neurosci 21:9856–9866.

Muschamp JW, Regina MJ, Hull EM, Winter JC, Rabin RA (2004) Lysergic acid diethylamide and [−]-2,5-dimethoxy-4-methylamphetamine increase extracellular glutamate in rat prefrontal cortex. Brain Res 1023:134–140.

Muthukumaraswamy SD, Carhart-Harris RL, Moran RJ, Brookes MJ, Williams TM, Errtizoe D, Sessa B, Papadopoulos A, Bolstridge M, Singh KD, Feilding A, Friston KJ, Nutt DJ (2013) Broadband Cortical Desynchronization Underlies the Human Psychedelic State. J Neurosci 33:15171–15183.

Nichols DE (2016) Psychedelics. Pharmacol Rev 68:264–355.

Oostenveld R, Fries P, Maris E, Schoffelen J-M (2010) FieldTrip: Open source software for advanced analysis of MEG, EEG, and invasive electrophysiological data. Comput Intell Neurosci 2011:156869.

Palhano-Fontes F et al. (2019) Rapid antidepressant effects of the psychedelic ayahuasca in treatment-resistant depression: a randomized placebo-controlled trial. Psychol Med 49:655–663.

Pallavicini C, Cavanna F, Zamberlan F, Fuente LA de la, Ilksoy Y, Perl YS, Arias M, Romero C, Carhart-Harris R, Timmermann C, Tagliazucchi E (2021) Neural and subjective effects of inhaled N,N-dimethyltryptamine in natural settings. J Psychopharmacol:026988112098138.

Pallavicini C, Vilas MG, Villarreal M, Zamberlan F, Muthukumaraswamy S, Nutt D, Carhart-Harris R, Tagliazucchi E (2019) Spectral signatures of serotonergic psychedelics and glutamatergic dissociatives. Neuroimage 200:281–291.

Paxinos, G. and Watson C. (2007) The Rat Brain in Stereotaxic Coordinates. Academic Press, London.

Pehek EA, Nocjar C, Roth BL, Byrd TA, Mabrouk OS (2006) Evidence for the Preferential Involvement of 5-HT2A Serotonin Receptors in Stress- and Drug-Induced Dopamine Release in the Rat Medial Prefrontal Cortex. Neuropsychopharmacology 31:265–277.

Rickli A, Moning OD, Hoener MC, Liechti ME (2016) Receptor interaction profiles of novel psychoactive tryptamines compared with classic hallucinogens. Eur Neuropsychopharmacol 26:1327–1337.

Scruggs JL, Schmidt D, Deutch AY (2003) The hallucinogen 1-[2,5-dimethoxy-4-iodophenyl]-2-aminopropane (DOI) increases cortical extracellular glutamate levels in rats. Neurosci Lett 346:137–140.

Sitaram BR, Lockett L, Talomsin R, Blackman GL, McLeod WR (1987) In vivo metabolism of 5-methoxy-N, N-dimethyltryptamine and N,N-dimethyltryptamine in the rat. Biochem Pharmacol 36:1509–1512.

Smith TL (1977) Increased synthesis of striatal dopamine by N,N-dimethyltryptamine. Life Sci 21:1597–1601.

Sohal VS, Zhang F, Yizhar O, Deisseroth K (2009) Parvalbumin neurons and gamma rhythms enhance cortical circuit performance. Nature 459:698–702.

Stoff DM, Moja EA, Gillin JC, Wyatt RJ (1978) Disruption of conditioned avoidance behavior by N, N-dimethyltryptamine (DMT) and stereotype by β-phenylethylamine (PEA): Animal models of attentional defects in schizophrenia. J Psychiatr Res 14:225–240.

Takahashi T, Takahashi K, Ido T, Yanai K, Iwata R, Ishiwata K, Nozoe S (1985) 11C-labelling of indolealkylamine alkaloids and the comparative study of their tissue distributions. Int J Appl Radiat Isot 36:965–969.

Timmermann C, Roseman L, Haridas S, Rosas FE, Luan L, Kettner H, Martell J, Erritzoe D, Tagliazucchi E, Pallavicini C, Girn M, Alamia A, Leech R, Nutt DJ, Carhart-Harris RL (2023) Human brain effects of DMT assessed via EEG-fMRI. Proc National Acad Sci 120:e2218949120.

Timmermann C, Roseman L, Schartner M, Milliere R, Williams LTJ, Erritzoe D, Muthukumaraswamy S, Ashton M, Bendrioua A, Kaur O, Turton S, Nour MM, Day CM, Leech R, Nutt DJ, Carhart-Harris RL (2019) Neural correlates of the DMT experience assessed with multivariate EEG. Sci Rep 9:16324.

Ungar F, Alivisatos SG (1976) Subsynaptosomal distribution, inhibition, and characterization of the binding of (14C) 5-OH-indole-3-acetaldehyde to brain preparations. Res Commun Chem Pathol Pharmacol 13:449–464.

Vanderwolf CH (1969) Hippocampal electrical activity and voluntary movement in the rat. Electroencephalogr Clin Neurophysiol 26:407–418.

Vargas MV, Dunlap LE, Dong C, Carter SJ, Tombari RJ, Jami SA, Cameron LP, Patel SD, Hennessey JJ, Saeger HN, McCorvy JD, Gray JA, Tian L, Olson DE (2023) Psychedelics promote neuroplasticity through the activation of intracellular 5-HT2A receptors. Science 379:700–706.

Vinck M, Oostenveld R, Wingerden M van, Battaglia F, Pennartz CMA (2011) An improved index of phase-synchronization for electrophysiological data in the presence of volume-conduction, noise and sample-size bias. Neuroimage 55:1548–1565.

Vollenweider FX, Kometer M (2010) The neurobiology of psychedelic drugs: implications for the treatment of mood disorders. Nat Rev Neurosci 11:642–651.

Vollenweider FX, Preller KH (2020) Psychedelic drugs: neurobiology and potential for treatment of psychiatric disorders. Nat Rev Neurosci 21:611–624.

Waldmeier PC, Maître L (1977) Neurochemical investigations of the interaction of N,N-dimethyltryptamine with the dopaminergic system in rat brain. Psychopharmacology 52:137–144.

Wojtas A, Bysiek A, Wawrzczak-Bargiela A, Szych Z, Majcher-Maślanka I, Herian M, Maćkowiak M, Gołembiowska K (2022) Effect of Psilocybin and Ketamine on Brain Neurotransmitters, Glutamate Receptors, DNA and Rat Behavior. Int J Mol Sci 23:6713.

Zangbar HS, Ghadiri T, Vafaee MS, Kalan AE, Fallahi S, Ghorbani M, Shahabi P (2020) Theta Oscillations Through Hippocampal/Prefrontal Pathway: Importance in Cognitive Performances. Brain Connectivity 10:157–169.

Figure Legends

Figure 1 Schematic showing the experimental timeline and histological verification of the neurochemical sampling sites. Panel (A) shows the experimental design and timeline. A perfusate sample was collected from both medial prefrontal cortex (mPFC) and somatosensory cortex (S1BF) for each 12.5 min epoch. DMT was administered at the start of the D1 epoch. EEG was collected continuously. Panel (B) shows the EEG montage (30 screw electrodes) to record high-density intracranial EEG and placement of open flow microperfusion (OFM) neurochemical sampling probes in mPFC and S1BF. Screw electrodes implanted above the sinus and cerebellum served as reference and ground electrodes, respectively. Schematics from the rat brain atlas (Paxinos and Watson, 2007) show coronal sections through mPFC (C) and S1BF (D) of the parietal region. Orange and turquoise cylinders represent the sampling length (1 mm) of the microperfusion probes implanted in mPFC and S1BF, respectively. The numbers associated with each stereotaxic map indicate the distance relative to bregma; positive numbers indicate anterior to bregma, and negative numbers indicate posterior to bregma. Representative cresyl violet stained coronal brain sections (30 µm) are shown for the histological verification of the probe placement in mPFC (C) and S1BF (D). fmi: forceps minor corpus callosum, IL: infralimbic cortex, L: lateral parietal association cortex, M: medial parietal association cortex, M2: secondary motor cortex, PrL: prelimbic region, RSD: retrosplenial dysgranular cortex, S1DZ: primary somatosensory cortex dysgranular zone, S1Tr: primary somatosensory trunk region.

Figure 2 Head twitch response after intravenous infusion of DMT. A) As compared to the low dose DMT (0.75 mg/kg), administration of DMT at medium (3.75 mg/kg) and high (7.5 mg/kg) doses resulted in significantly fewer head twitches. B) There were no differences in number of head twitches after any of the three doses between male and female rats. Black dots show values

for individual rats. Error bars indicate standard error of the mean (s.e.m.). A linear mixed model was used to compare the number of head twitches between doses of DMT. The p values were adjusted for multiple comparisons with Tukey test. *p<0.05.

Figure 3 DMT levels in medial prefrontal cortex and somatosensory cortex before, during, and after intravenous administration of DMT. Panels (A) and (B) show log (base 10) transformed raw concentrations (nM) of DMT in medial prefrontal cortex (mPFC) and somatosensory cortex (S1BF) for each epoch, respectively. Panels (C) and (D) show the concentration of DMT in mPFC and S1BF after combining the epochs W1-W4 as "wake", D1-D2 as "drug", D3-D5 as "post-drug", and D6-D7 as "recovery". The data are shown as change (log) from wake. Statistical analyses compared each epoch (D1-D7) in (A) and (B), and drug, post-drug, and recovery in (C) and (D) to the wake epoch. The DMT concentration remained significantly elevated until the D5 epoch for the low dose and remained significantly higher for medium and high doses throughout the duration of experiment. Orange circles represent the low dose (0.75 mg/kg), green triangles represent the medium dose (3.75 mg/kg), and magenta squares represent the high dose (7.5 mg/kg). A linear mixed model was used to compare the levels of recoverable DMT between epochs. The p values were adjusted for multiple comparisons via Dunnett's test. *p<0.05 with asterisks color coded to match the symbol/dose. s.e.m.: standard error of the mean.

Figure 4 Intravenous administration of DMT increased the levels of 5-HT and dopamine in medial prefrontal cortex and somatosensory cortex. Panels (A) and (B) show the effect of intravenous administration of DMT on 5-HT levels in medial prefrontal cortex (mPFC) and somatosensory cortex (S1BF), respectively. In both brain regions, medium and high doses of DMT caused 5-HT to increase during the drug epoch whereas the low dose DMT resulted in decreased 5-HT levels during the recovery epoch. Panels (C) and (D) show the effect of intravenous

administration of DMT on dopamine (DA) levels in mPFC and S1BF, respectively. The high dose of DMT caused DA to increase during the drug epoch in both brain regions. Orange circles represent the low dose (0.75 mg/kg), green triangles represent the medium dose (3.75 mg/kg), and magenta squares represent the high dose (7.5 mg/kg). A linear mixed model was used to compare the levels of 5-HT (A-B) or DA (C-D) between states. The p values were adjusted for multiple comparisons via Dunnett's test. *$p<0.05$ with asterisks color coded to match the symbol/dose. s.e.m.: standard error of the mean.

Figure 5 Neurochemical changes in medial prefrontal cortex and somatosensory cortex after intravenous administration of DMT. Log (base 10) transformed raw concentrations of neurochemicals quantified from medial prefrontal cortex (mPFC) and somatosensory cortex (S1BF) were averaged into wake (W), drug (D), post-drug (P), and recovery (R) bins. No significant changes, as compared to the wake epoch, were observed during the drug epoch for any of the analytes in either brain region. Orange circles represent the low dose (0.75 mg/kg), green triangles represent the medium dose (3.75 mg/kg), and magenta squares represent the high dose (7.5 mg/kg). A linear mixed model was used to compare levels of each analyte between states. The p values were adjusted for multiple comparisons via Dunnett's test. *$p<0.05$ with asterisks color coded to match the symbol/dose. s.e.m.: standard error of the mean.

Figure 6 Relationship between the levels of recoverable DMT and levels of 5-HT and dopamine in medial prefrontal cortex and somatosensory cortex after intravenous administration of DMT. Correlation analyses using log (base 10) transformed neurochemical concentrations during D1-D7 epochs for low (0.75 mg/kg - orange), medium (3.75 mg/kg - green), and high (7.5 mg/kg – magenta) doses of DMT. Spearman's rank correlation was used to calculate correlation coefficients (ρ) between serotonin (5-HT) and DMT levels in medial prefrontal cortex

mPFC (A) and somatosensory cortex (S1BF) (B), and dopamine (DA) and DMT levels in mPFC (C) and S1BF (D). Regression lines are shown for each dose with shaded areas representing 95% confidence intervals. Positive correlations were observed between 5-HT and recoverable DMT and between DA and recoverable DMT in both brain regions. The p values were calculated via two-tailed t-tests. The correlation coefficients (ρ) are shown for each plot, with colors corresponding to dose.

Figure 7 Basal levels of serotonin, dopamine, and endogenous DMT in medial prefrontal cortex and somatosensory cortex. Basal values for 5-HT, dopamine, and DMT levels are shown as the average of the four wake samples collected during the baseline wake (pre-DMT infusion) state. The levels of DMT are within the range of 5-HT and DA in both brain regions. Error bars indicate standard error of mean (s.e.m.).

Figure 8 Effect of intravenous administration of DMT on EEG spectral power. The changes in EEG spectral power at selected frequency bands were determined by comparing the relative spectral power in the averaged baseline wake epoch to that in each of the 7 drug (D1-D7) epochs. There was increased delta and decreased theta relative power during the D1 epoch following the low (0.75mg/kg – Orange circles) and medium (3.75mg/kg – Green triangles) doses, and during the D2 epoch following the high dose (7.5mg/kg – Magenta squares). During D1, a significant increase in medium gamma power was observed after the medium and high doses of DMT, and increase in high gamma power after all three doses. Low gamma power increased in later post-infusion epochs (D4-D7) across doses. A linear mixed model was used to compare EEG relative power between states. The p values were adjusted for multiple comparisons via Dunnett's test. *$p<0.05$ with asterisks color coded to match the symbol/dose. s.e.m.: standard error of the mean.

Figure 9 Effect of intravenous administration of DMT on delta- and theta functional connectivity. Adjacency matrices show the normalized weighted phase lag index (wPLI) value after low (0.75 mg/kg), medium (3.75 mg/kg), and high (7.5 mg/kg) doses of intravenous DMT for all channel pairs during wake and each drug (D1-D7) epoch for delta (1-4 Hz) and theta (4-10 Hz) bands. Global delta wPLI decreased after the administration of low and medium doses of DMT during the D1 epoch, and after the high dose for the D2 epoch. Global theta wPLI increased after the high dose DMT during D1, primarily in frontal-posterior electrode pairs, and subsequently decreased during D2. Warmer colors indicate greater wPLI values (i.e., greater functional connectivity) and cooler colors indicate lower wPLI values. A linear mixed model was used to compare global wPLI between states. The p values were adjusted for multiple comparisons via Dunnett's test. *$p<0.05$

Figure 10 Effect of intravenous administration of DMT on gamma functional connectivity. Adjacency matrices show the normalized weighted phase lag index (wPLI) value after low (0.75 mg/kg), medium (3.75 mg/kg), and high (7.5 mg/kg) doses of intravenous DMT for all channel pairs during wake and each drug (D1-D7) epoch for low (25–55 Hz), medium (65-115 Hz), and high (125-155 Hz) gamma bands. DMT administration increased functional connectivity in each of the three gamma bands in a dose-dependent manner, with higher doses causing more persistent changes, starting with the D1 epoch. Increases in low gamma connectivity dominated in parietal-occipital electrode pairs, medium gamma connectivity increases occurred in parietal electrodes, and high gamma connectivity increases were observed in frontal-parietal electrode pairs. Warmer colors indicate greater wPLI values (i.e., greater functional connectivity) and cooler colors indicate lower wPLI values. A linear mixed model was used to compare global wPLI between states. The p values were adjusted for multiple comparisons via Dunnett's test. *$p<0.05$

Author Contributions

N.G.G. and D.P. designed the study; N.G.G. performed surgeries, experiments, statistical analysis, and neurochemical analysis; E.R.H. and A.N. performed EEG analysis; R.T.K. and Y.K. assisted with neurochemical analyses: N.G.G., G.A.M., and D.P. wrote the manuscript and interpreted the data. All authors contributed to the final draft of the article.

Funding

This research was supported by the National Institutes of Health Grant R01 GM111293 to D.P., RF1-NS128522 to R.T.K., and funding from the Michigan Psychedelic Center and Department of Anesthesiology, University of Michigan Medical School, Ann Arbor, Michigan.

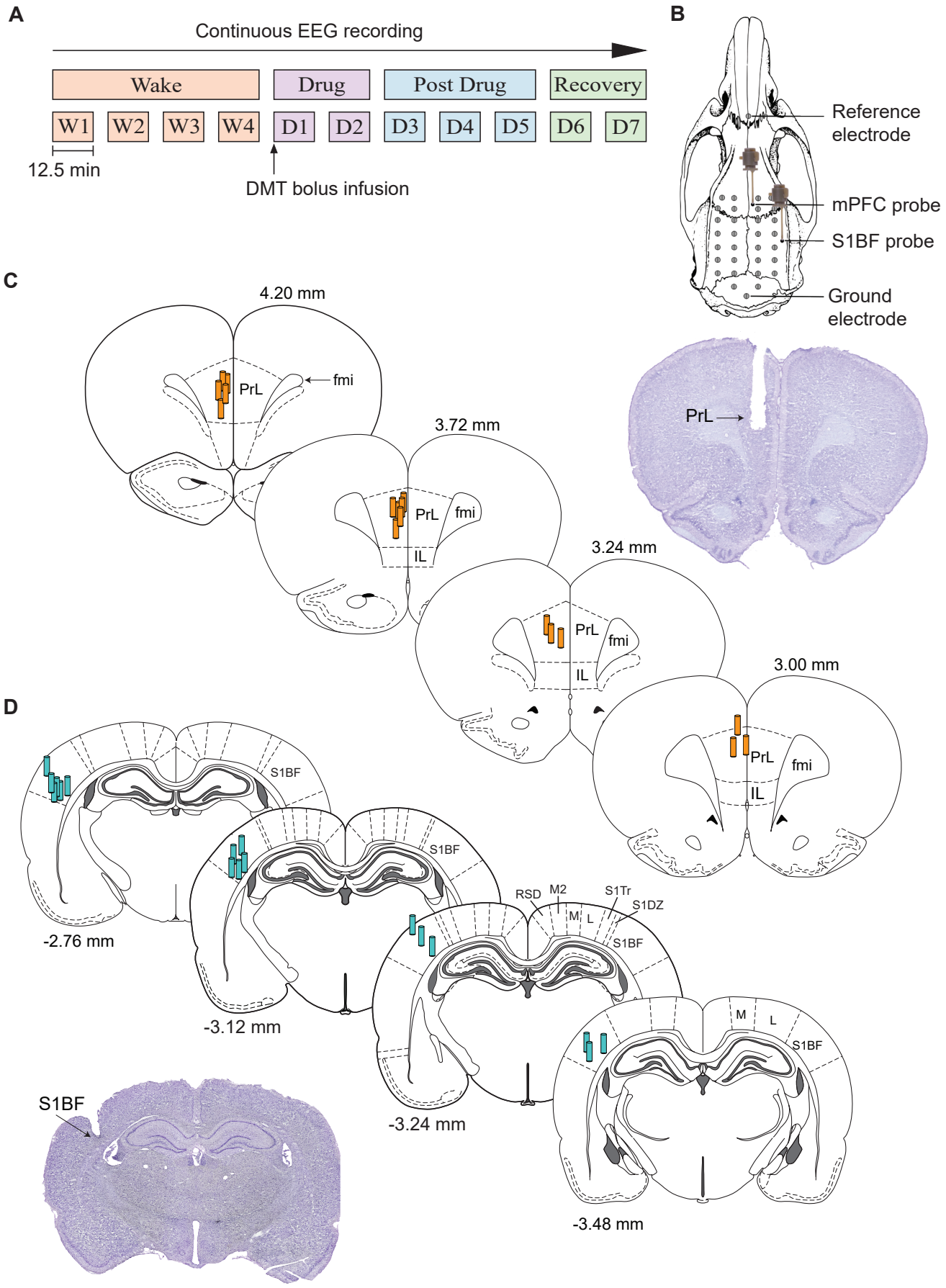
A
Continuous EEG recording
Wake
Drug
Post Drug
Recovery
W1
W2
W3
W4
D1
D2
D3
D4
D5
D6
D7
12.5 min
DMT bolus infusion
B
Reference electrode
mPFC probe
S1BF probe
Ground electrode
C
4.20 mm
PrL
fmi
3.72 mm
PrL
fmi
IL
3.24 mm
PrL
fmi
IL
3.00 mm
PrL
fmi
IL
PrL
D
S1BF
-2.76 mm
S1BF
-3.12 mm
RSD
M2
S1Tr
S1DZ
M
L
S1BF
-3.24 mm
M
L
S1BF
-3.48 mm
S1BF

Figure 1

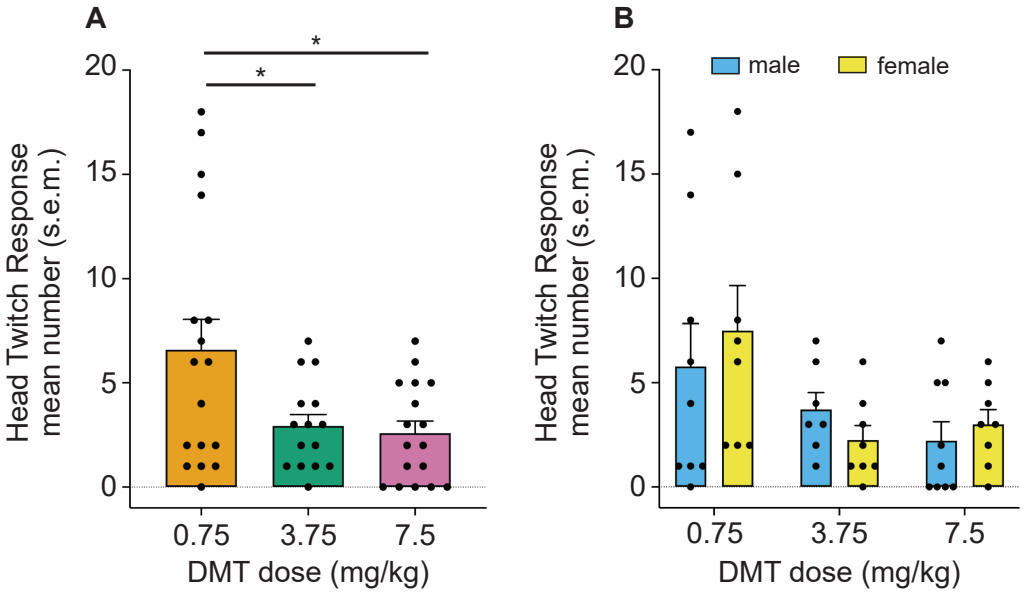
A
B
male
female
Head Twitch Response
mean number (s.e.m.)
20
15
10
5
0
*
*
0.75
3.75
7.5
DMT dose (mg/kg)

Figure 2

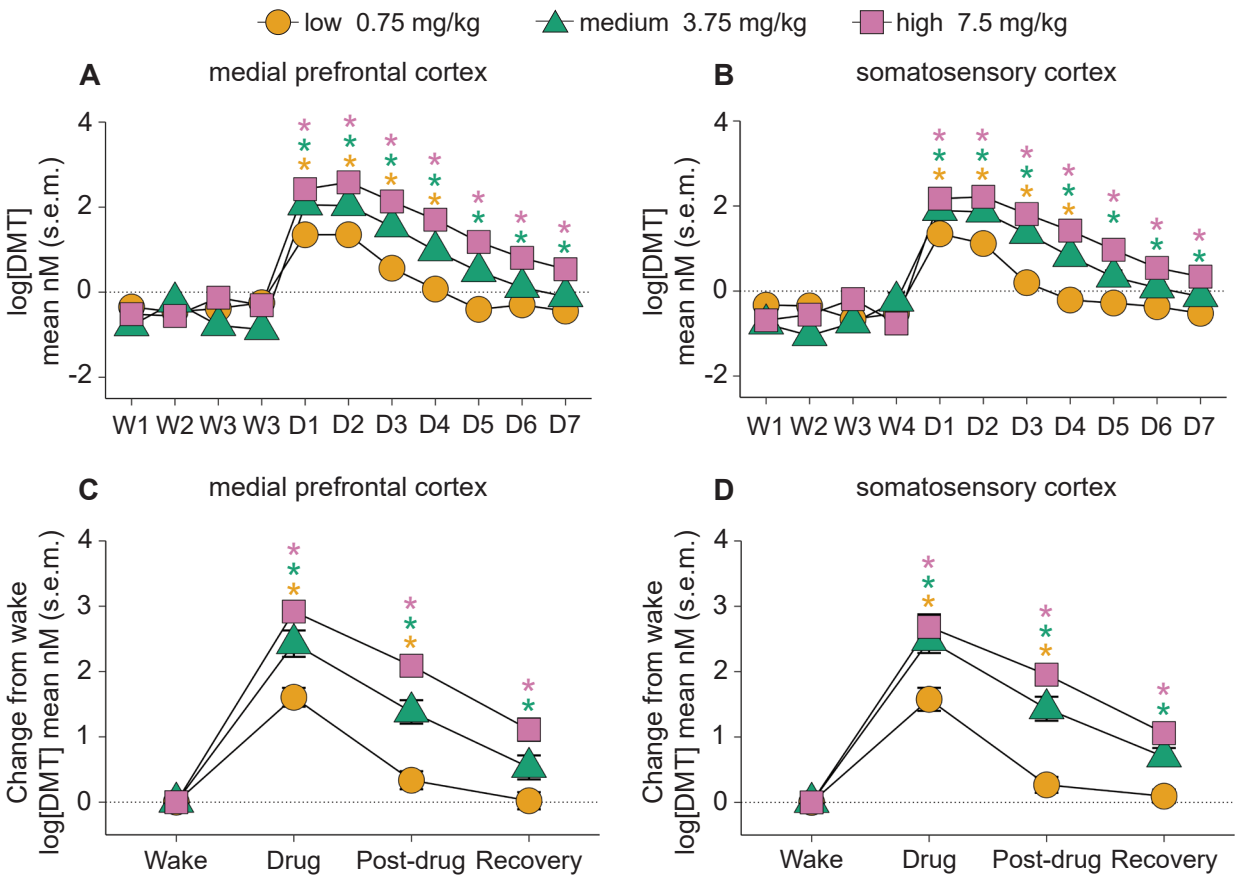
low 0.75 mg/kg
medium 3.75 mg/kg
high 7.5 mg/kg
A
medial prefrontal cortex
log[DMT]
mean nM (s.e.m.)
W1 W2 W3 W3 D1 D2 D3 D4 D5 D6 D7
B
somatosensory cortex
log[DMT]
mean nM (s.e.m.)
W1 W2 W3 W4 D1 D2 D3 D4 D5 D6 D7
C
medial prefrontal cortex
Change from wake
log[DMT] mean nM (s.e.m.)
Wake
Drug
Post-drug
Recovery
D
somatosensory cortex
Change from wake
log[DMT] mean nM (s.e.m.)
Wake
Drug
Post-drug
Recovery

Figure 3

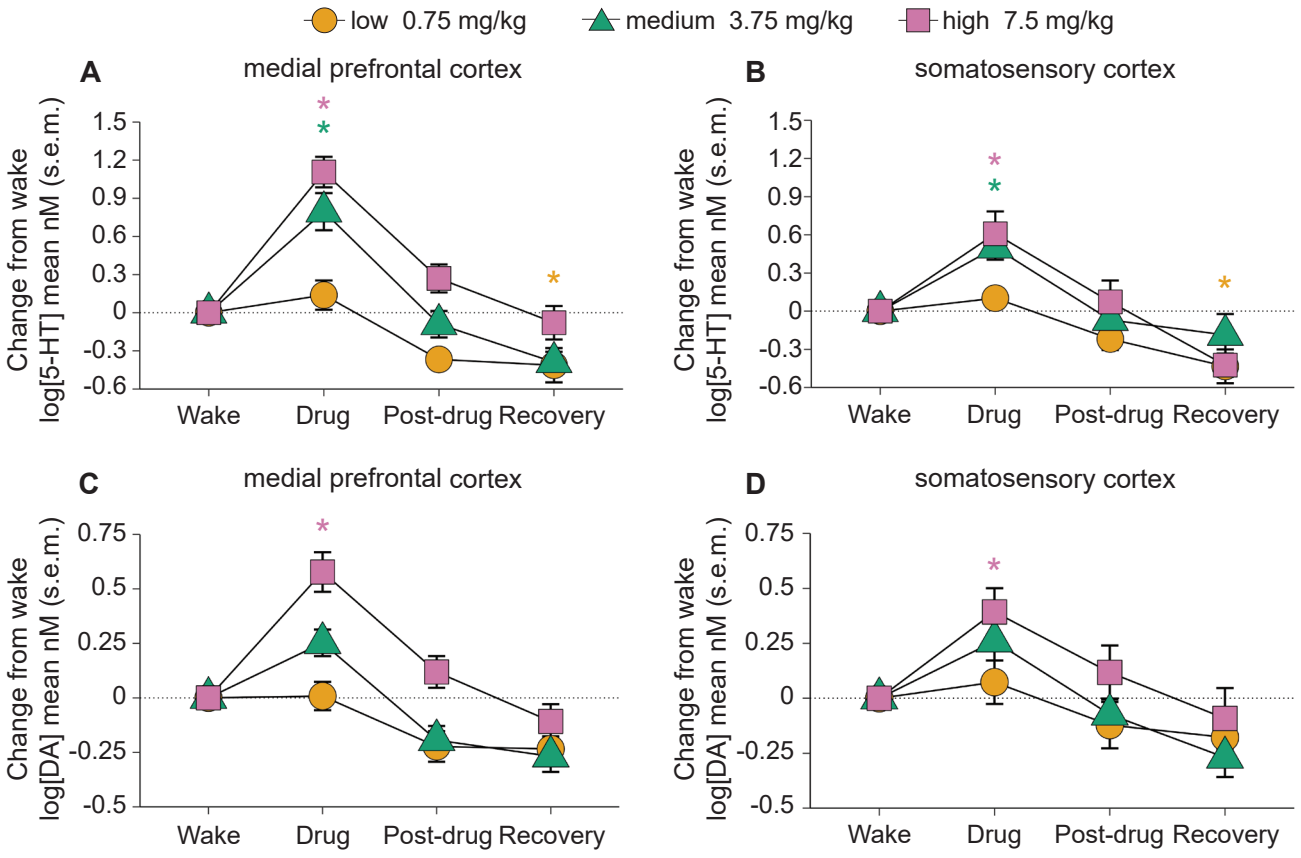
low 0.75 mg/kg
medium 3.75 mg/kg
high 7.5 mg/kg
A
medial prefrontal cortex
Change from wake
log[5-HT] mean nM (s.e.m.)
1.5
1.2
0.9
0.6
0.3
0
-0.3
-0.6
Wake
Drug
Post-drug
Recovery
B
somatosensory cortex
Change from wake
log[5-HT] mean nM (s.e.m.)
C
medial prefrontal cortex
Change from wake
log[DA] mean nM (s.e.m.)
0.75
0.5
0.25
0
-0.25
-0.5
D
somatosensory cortex
Change from wake
log[DA] mean nM (s.e.m.)

Figure 4

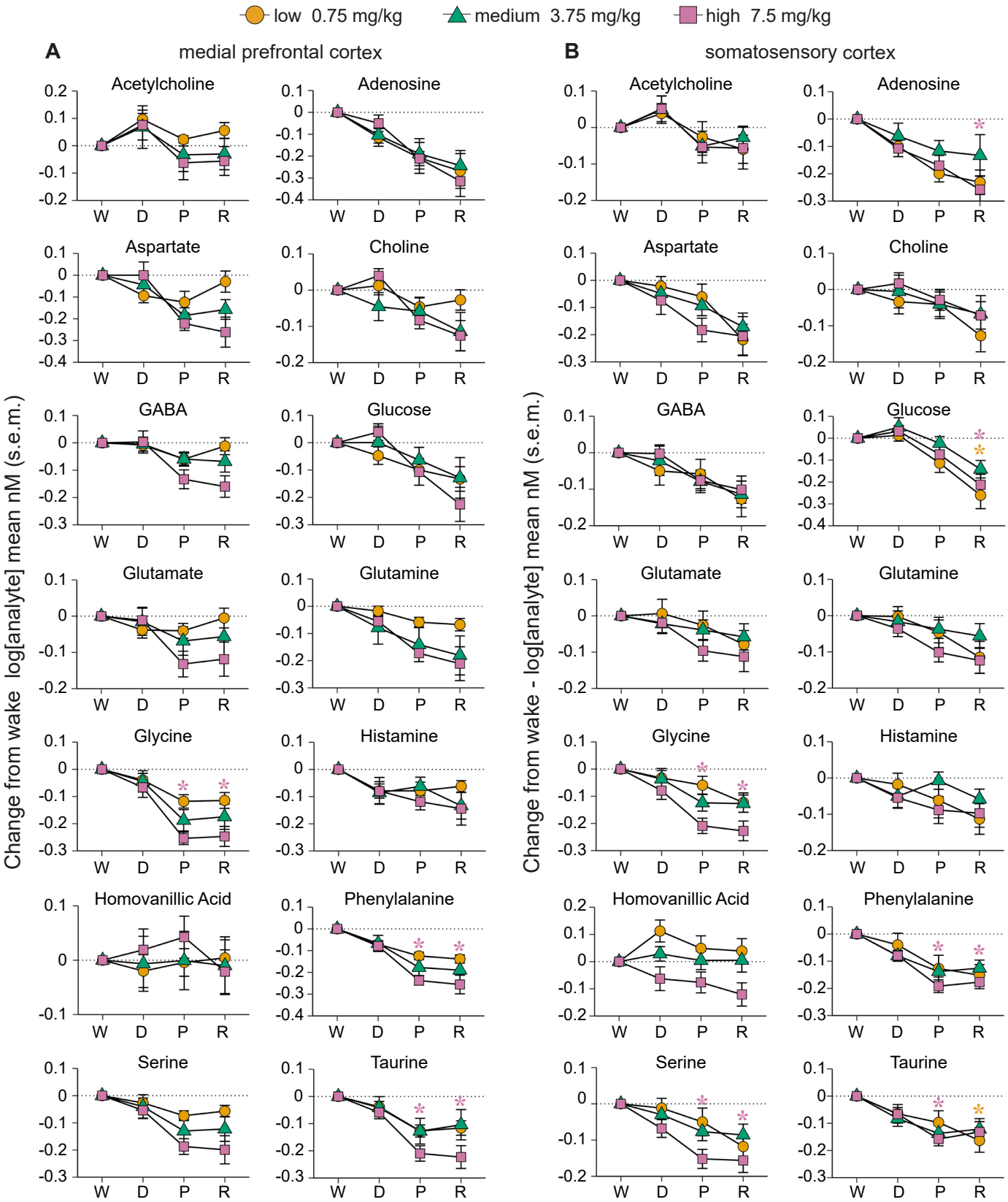
low 0.75 mg/kg
medium 3.75 mg/kg
high 7.5 mg/kg
A
medial prefrontal cortex
B
somatosensory cortex
Acetylcholine
Adenosine
Aspartate
Choline
GABA
Glucose
Glutamate
Glutamine
Glycine
Histamine
Homovanillic Acid
Phenylalanine
Serine
Taurine
W D P R
Change from wake - log[analyte] mean nM (s.e.m.)

Figure 5

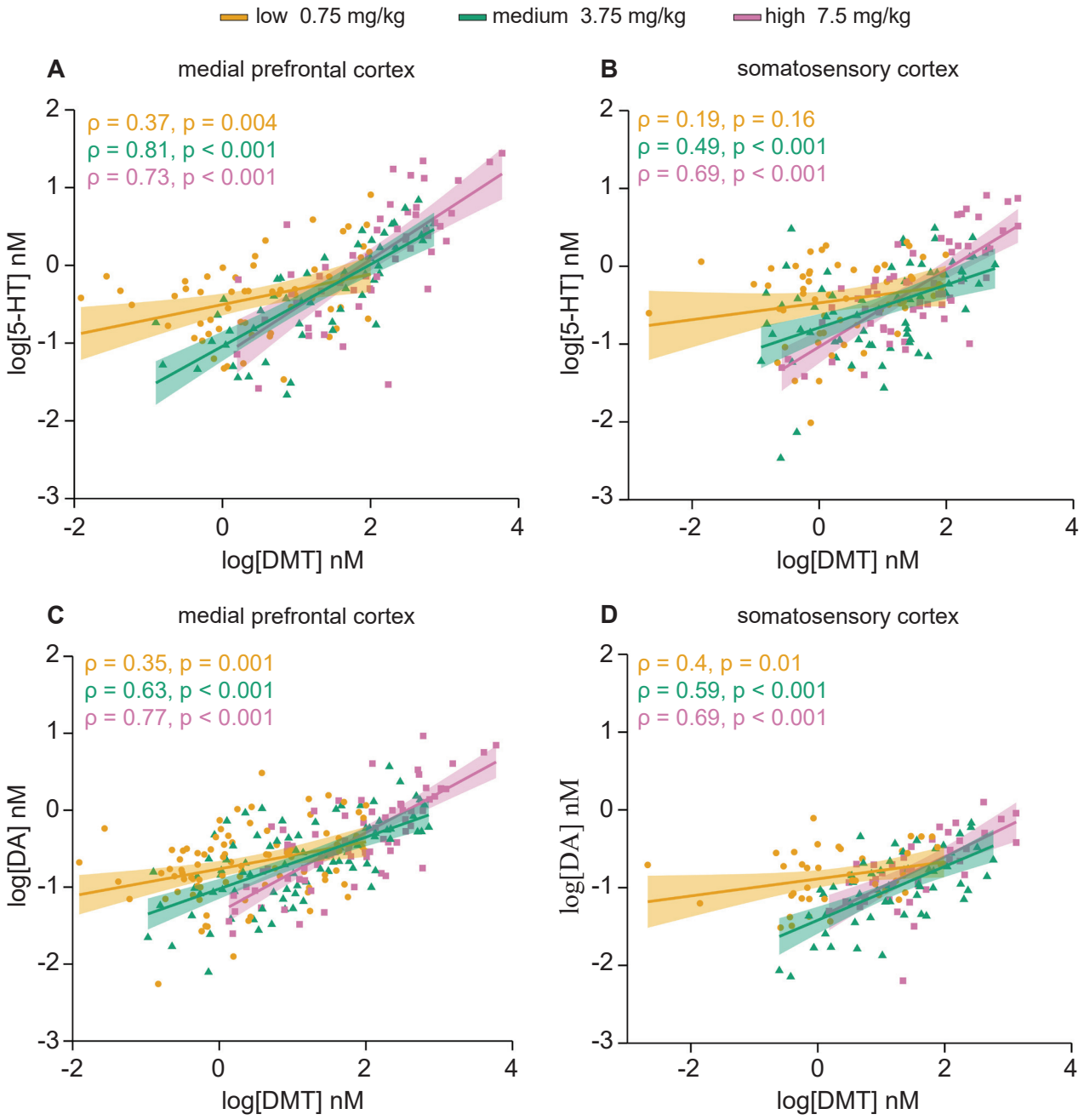
low 0.75 mg/kg
medium 3.75 mg/kg
high 7.5 mg/kg
A
medial prefrontal cortex
ρ = 0.37, p = 0.004
ρ = 0.81, p < 0.001
ρ = 0.73, p < 0.001
log[5-HT] nM
log[DMT] nM
B
somatosensory cortex
ρ = 0.19, p = 0.16
ρ = 0.49, p < 0.001
ρ = 0.69, p < 0.001
log[5-HT] nM
log[DMT] nM
C
medial prefrontal cortex
ρ = 0.35, p = 0.001
ρ = 0.63, p < 0.001
ρ = 0.77, p < 0.001
log[DA] nM
log[DMT] nM
D
somatosensory cortex
ρ = 0.4, p = 0.01
ρ = 0.59, p < 0.001
ρ = 0.69, p < 0.001
log[DA] nM
log[DMT] nM

Figure 6

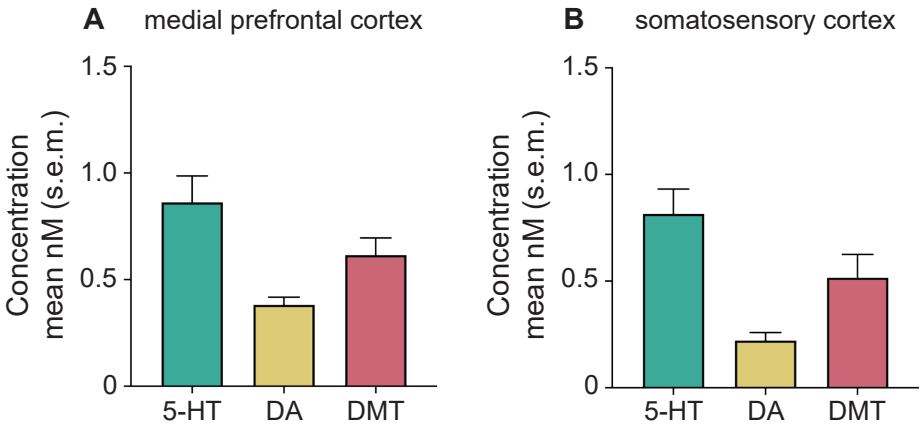
A
medial prefrontal cortex
B
somatosensory cortex
Concentration
mean nM (s.e.m.)
1.5
1.0
0.5
0
5-HT
DA
DMT

Figure 7

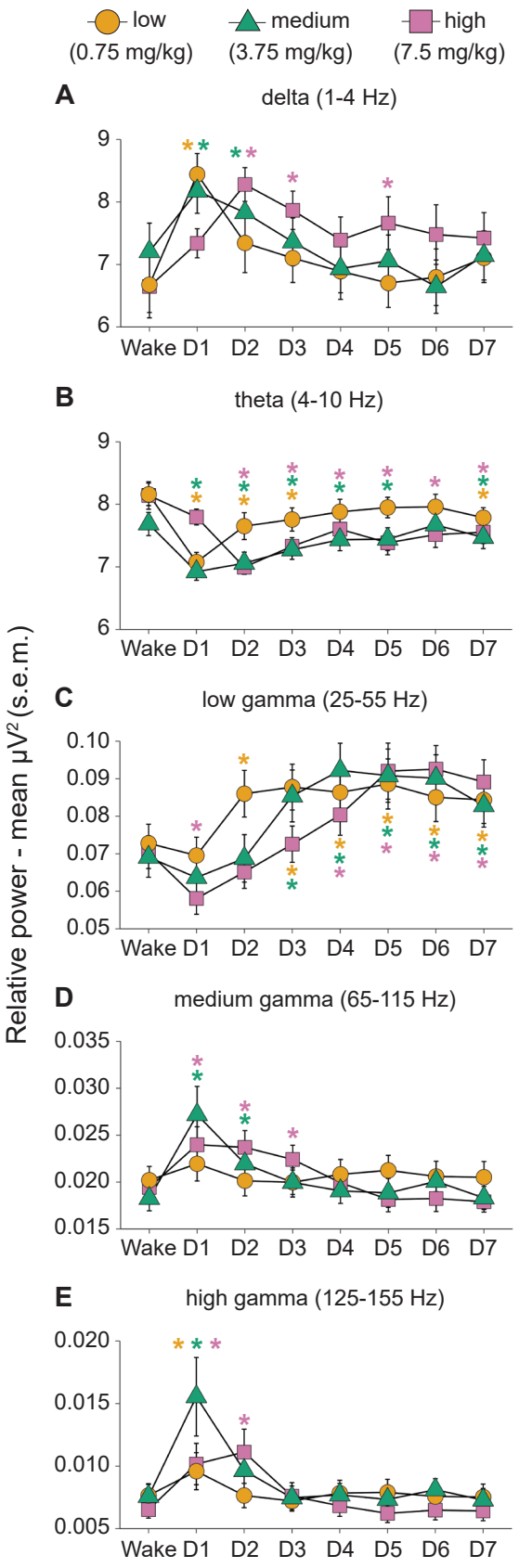
low
(0.75 mg/kg)
medium
(3.75 mg/kg)
high
(7.5 mg/kg)
A
delta (1-4 Hz)
B
theta (4-10 Hz)
C
low gamma (25-55 Hz)
D
medium gamma (65-115 Hz)
E
high gamma (125-155 Hz)
Relative power - mean μV² (s.e.m.)
Wake D1 D2 D3 D4 D5 D6 D7

Figure 8

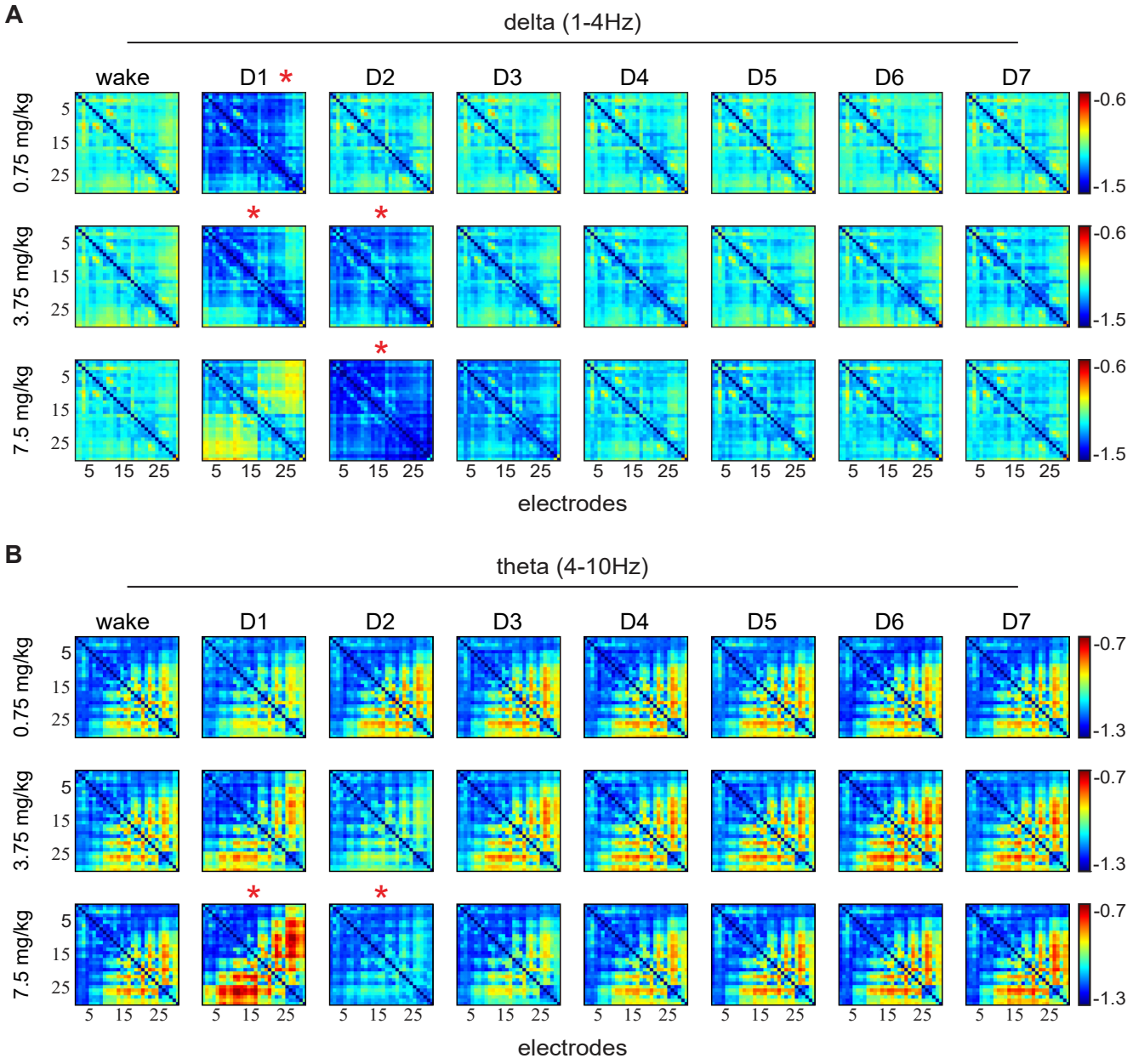
A
delta (1-4Hz)
wake
D1
D2
D3
D4
D5
D6
D7
0.75 mg/kg
3.75 mg/kg
7.5 mg/kg
5
15
25
-0.6
-1.5
electrodes
B
theta (4-10Hz)
-0.7
-1.3

Figure 9

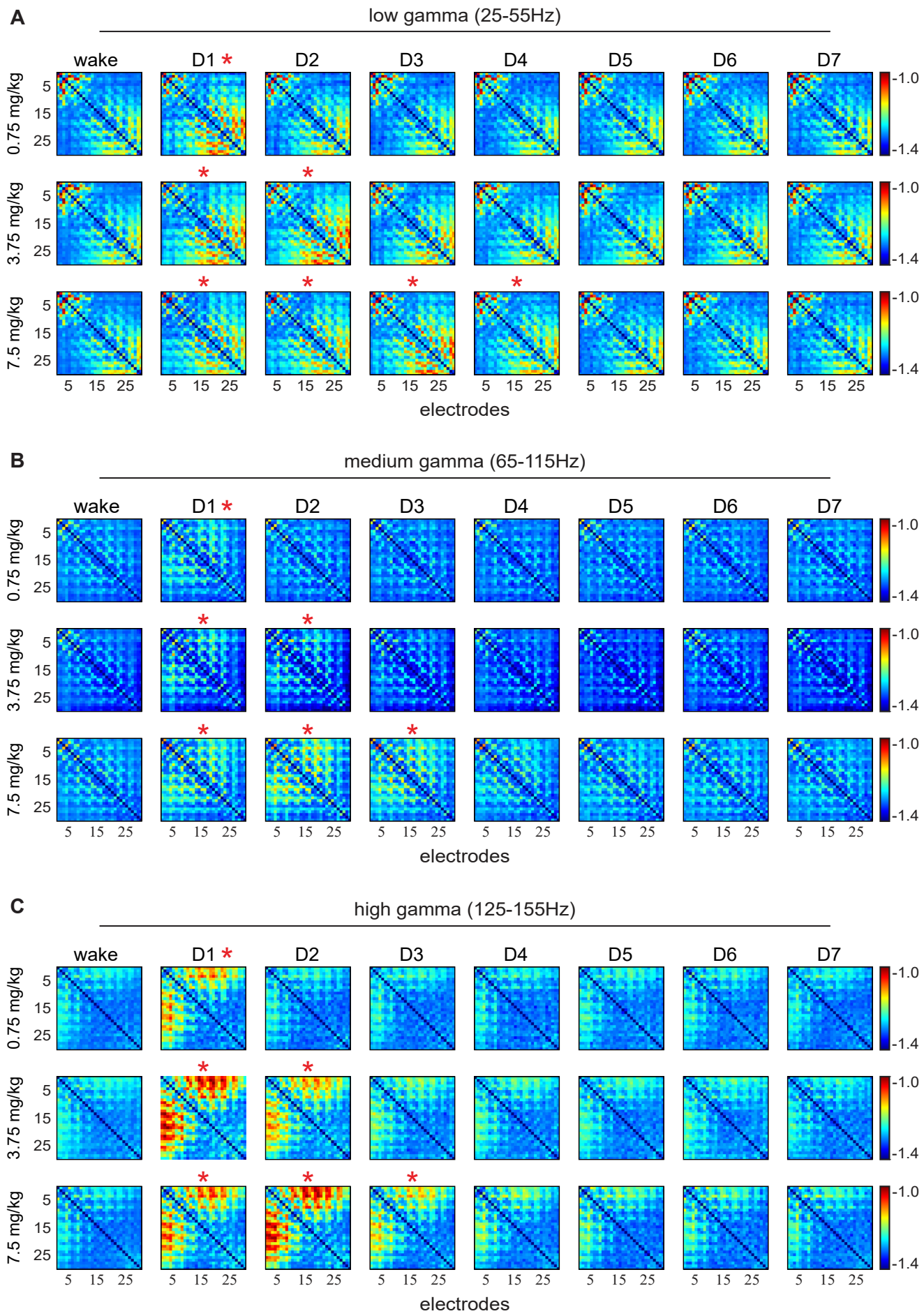
A
low gamma (25-55Hz)
wake
D1
D2
D3
D4
D5
D6
D7
0.75 mg/kg
3.75 mg/kg
7.5 mg/kg
5
15
25
-1.0
-1.4
electrodes
B
medium gamma (65-115Hz)
C
high gamma (125-155Hz)

Figure 10